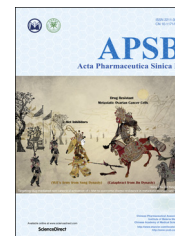




Chinese Pharmaceutical Association
Institute of Materia Medica, Chinese Academy of Medical Sciences

Acta Pharmaceutica Sinica B

www.elsevier.com/locate/apsb
www.sciencedirect.com



ORIGINAL ARTICLE

Targeting slug-mediated non-canonical activation of c-Met to overcome chemo-resistance in metastatic ovarian cancer cells



Linlin Chang^{a,†}, Yan Hu^{a,†}, Yingying Fu^{a,†}, Tianyi Zhou^a, Jun You^b,
Jiamin Du^a, Lin Zheng^a, Ji Cao^a, Meidan Ying^a, Xiaoyang Dai^a,
Dan Su^b, Qiaojun He^a, Hong Zhu^{a,*}, Bo Yang^{a,*}

^aZhejiang Province Key Laboratory of Anti-Cancer Drug Research, College of Pharmaceutical Sciences, Zhejiang University, Hangzhou 310058, China

^bZhejiang Cancer Hospital, Hangzhou 310022, China

Received 3 January 2019; received in revised form 8 February 2019; accepted 1 March 2019

KEY WORDS

Slug;
c-Met;
Drug resistance;
Ovarian cancer;
XL184

Abstract Metastasis-associated drug resistance accounts for high mortality in ovarian cancer and remains to be a major barrier for effective treatment. In this study, SKOV3/T4, a metastatic subpopulation of ovarian cancer SKOV3 cells, was enriched to explore potential interventions against metastatic-associated drug resistance. Quantitative genomic and functional analyses were performed and found that slug was significantly increased in the SKOV3/T4 subpopulation and contributed to the high resistance of SKOV3/T4. Further studies showed that slug activated c-Met in a ligand-independent manner due to elevated levels of fibronectin and provoked integrin αV function, which was confirmed by the significant correlation of slug and p-Met levels in 121 ovarian cancer patient samples. Intriguingly, c-Met inhibitor(s) exhibited greatly enhanced anti-cancer effects in slug-positive ovarian cancer models both *in vitro* and *in vivo*. Additionally, IHC analyses revealed that slug levels were highly correlated with reduced survival of ovarian cancer patients. Taken together, this study not only uncovers the critical roles of slug in drug resistance in ovarian cancer but also highlights a promising therapeutic strategy by

Abbreviations: EMT, epithelial-mesenchymal transition; FBS, fetal bovine serum; PVDF, polyvinylidene fluoride; cDNA, complementary DNA; CO₂, carbon dioxide; DMEM, Dulbecco's modified Eagle's medium; ELISA, enzyme-linked immunosorbent assay; IHC, immunohistochemistry; SDS, sodium dodecyl sulfate; TGF- β , transforming growth factor-beta; HGF, hepatocyte growth factor; PFS, progression-free survival; OS, overall survival; PPS, postprogression survival; ITGA5, integrin subunit alpha 5; PBS, phosphate buffered solution; EGFR, epidermal growth factor receptor; VEGFR, kinase insert domain receptor; qRT-PCR, quantitative reverse transcription polymerase chain reaction

*Corresponding authors. Tel./fax: +86 571 88208400.

E-mail addresses: hongzhu@zju.edu.cn (Hong Zhu), yang924@zju.edu.cn (Bo Yang).

[†]These authors made equal contributions to this study.

Peer review under responsibility of Institute of Materia Medica, Chinese Academy of Medical Sciences and Chinese Pharmaceutical Association.

<https://doi.org/10.1016/j.apsb.2019.03.001>

2211-3835 © 2019 Chinese Pharmaceutical Association and Institute of Materia Medica, Chinese Academy of Medical Sciences. Production and hosting by Elsevier B.V. This is an open access article under the CC BY-NC-ND license (<http://creativecommons.org/licenses/by-nc-nd/4.0/>).

targeting the noncanonical activation of c-Met in slug-positive ovarian cancer patients with poor prognosis.

© 2019 Chinese Pharmaceutical Association and Institute of Materia Medica, Chinese Academy of Medical Sciences. Production and hosting by Elsevier B.V. This is an open access article under the CC BY-NC-ND license (<http://creativecommons.org/licenses/by-nc-nd/4.0/>).

1. Introduction

Ovarian cancer is the most common cause of gynecological cancer-associated death¹. Since 60% of ovarian cancer patients are diagnosed with late-stage tumors that have already metastasized beyond the ovaries, systematic chemotherapy has been a general standard treatment. However, these metastatic cancer cells are highly resistant to first-line therapeutic agents including platinum, adriamycin, etc., which ultimately leads to treatment failure and patient death². Accordingly, metastasis-associated drug resistance remains to be a major barrier to effective treatment in ovarian cancer patients, and the exploration of effective therapeutic interventions based on the underlying mechanisms is an urgent need.

Emerging evidence suggests that intratumoral heterogeneity contributes to the development of drug resistance in a variety of solid tumors including ovarian cancer^{1,3}, and cancer cells harboring high metastasis potential within the tumor cell population may represent the one of the most important patterns of intratumoral heterogeneity^{4,5}. To date, most studies that have enriched metastatic subpopulations inside a tumor mass or cancer cell lines with heterogeneity generally aim to explore the key factors promoting metastasis^{5,6}. Thus the mechanisms underlying metastasis-associated drug resistance remain largely elusive. In our study, a subpopulation of ovarian cancer cells with high metastatic potential was enriched. Interestingly, this subpopulation distinctly lost its susceptibility to a variety of anti-cancer drugs including first-line chemotherapeutic agents. This finding is in line with the coexistence of metastatic- and resistant-potential in a same cell population inside a tumor, which is particularly observed in highly metastatic ovarian cancer. Given the close link between metastasis potential and the loss of susceptibility, we were inspired to speculate that the factors mediating drug resistance might overlap with critical signaling pathways in metastasis.

Epithelial–mesenchymal transition (EMT) is essential for the acquisition of cellular plasticity, which promotes metastasis^{7,8}. Recent findings have also unveiled its important roles in the acquirement of drug resistance. Mounting evidence indicates that transcriptional reprogramming *via* transcription factors consisting of three superfamilies, including the snail, bHLH, and ZEB factors, plays critical roles in the progress of EMT. Slug (snail2), a member of the snail family, regulates the cellular plasticity necessary for tumor metastasis by repressing E-cadherin and increasing fibronectin as well as vimentin^{9,10}. Accumulating reports show that in addition to metastasis, slug also conferred resistance to cisplatin¹¹, gemcitabine¹², tamoxifen¹³ and tyrosine kinase inhibitors¹⁴ in ovarian cancer, pancreatic cancer, breast cancer and lung cancer cells. Interfering with slug expression through RNA silencing in EMT-like resistant cells could significantly increase the efficacy of anti-cancer drugs, indicating that targeting slug-associated signaling may overcome the drug resistance.

Even though slug expression could predict chemo-resistance, the unraveled knowledge of its downstream signaling greatly hinders the feasibility of targeting slug to overcome treatment resistance.

Here, in this study, we applied combined transcriptional profiling and functional analyses to the enriched metastatic subpopulation of ovarian cancer cells aiming to not only unearth the important roles played by EMT regulator slug in the development of heterogeneity and drug resistance toward a panel of chemotherapeutic agents in ovarian cancer, but also establish the causal link between over-expressed slug and the activation of c-Met, a receptor tyrosine kinase. Blocking the aberrant activation of c-Met with kinase inhibitors could significantly ameliorate the chemo-resistance of the enriched metastatic subpopulation, thus offering an effective strategy for slug-positive resistant ovarian cancer cells.

2. Methods and materials

2.1. Cell culture

Human ovarian cancer SKOV3 cells were purchased from Shanghai Institutes for Biological Sciences (Cell Bank of China Science Academy, Shanghai, China). SKOV3 and the enriched metastatic subpopulation SKOV3/T4 were maintained in RPMI 1640 medium (Gibco, Grand Island, New York, USA) supplied with penicillin (100 U/mL), streptomycin (100 µg/mL) (Sigma–Aldrich, St. Louis, MO, USA) and 10% fetal bovine serum (FBS, Gibco) at 37 °C in a humidified atmosphere containing 5% carbon dioxide (CO₂). The cells were authenticated by using DNA fingerprinting (variable number of tandem repeats), confirming that no cross-contamination occurred during this study.

2.2. Enrichment of the highly metastatic SKOV3/T4 subpopulation

After starvation for 12 h, an SKOV3 cell suspension without FBS (200 µL, 1×10^5 cells) was placed in the upper chamber, while the lower chamber contained 600 µL of culture medium containing 10% FBS. Cells that migrated to the lower chamber were designated as SKOV3/T1 and subjected to the next cycle of migration and enrichment. SKOV3/T4 cells were obtained by repeating the above experiments 3 more times.

2.3. Wound-healing assay

SKOV3 and SKOV3/T4 cells were seeded in 24-well plates. After starvation overnight, a wound was generated using a pipette tip to make a straight scratch. The cells were treated with or without drug and cultured for an indicated time. Pictures were taken to assess the ability of the cells to migrate to the clear section.

2.4. Migration assay

SKOV3 and SKOV3/T4 cell suspensions (200 µL, 1×10^5 cells) were placed in the upper chamber. The cells that migrated to the lower chamber were fixed with 75% precooled alcohol for 30 min

followed by staining with 0.1% crystal violet (Sigma–Aldrich) for 10 min. The cells were then photographed under a microscope.

2.5. Gene transfection and RNA interference

Cells were seeded onto 6-well plates and transfected using Oligofectamine (Thermo Fisher Scientific, Waltham, MA, USA) or X-treme GENE HP DNA Transfection Reagent (Roche, 6366546001) according to the manufacturer's instructions. All the siRNAs were obtained from GenePharma Co., Ltd. (Shanghai, China). The targeting sequences are shown in [Supporting Information Table S1](#).

2.6. Immunofluorescence

Cells were plated onto culture slides, fixed with 4% paraformaldehyde and permeabilized with 0.1% Triton X-100 (Beyotime, Haimen, China), washed twice with phosphate buffered solution (PBS), and blocked with 3% BSA for 30 min. The cells were then probed with the corresponding primary and secondary antibodies. The cells were then stained with DAPI (Invitrogen, Waltham, MA, USA) for 5 min and photographed with a fluorescence confocal microscope.

2.7. Immunohistochemistry

Paraffin-embedded ovarian cancer orthotopic tumor tissue samples were processed by the following steps: dewaxing, rehydrating, and subjecting to microwave with citrate buffer pH 6.0 for staining. Then, Histostain-Plus Kit was then used according to the manufacturer's instructions (Thermo Fisher Scientific).

2.8. Quantitative reverse-transcriptase polymerase chain reaction

RNA was extracted with the EasyPure RNA kit (Transgen Biotech, Beijing, China) and Complementary DNA (cDNA) was obtained by RNA reverse transcription using the TransScript One-Step gDNA Removal and cDNA Synthesis SuperMix kit (Transgen, Beijing, China). This was followed by SYBR[®]-Green real-time PCR (Qiagen, Valencia, CA, USA). The cDNA pools were amplified using a 96-well Thermal Cycler (Applied Biosystems, Foster, CA, USA) with the primers (Biosune, Shanghai, China) provided in [Supporting Information Table S2](#).

2.9. Western blot analysis

Protein samples were separated by sodium dodecyl sulfate polyacrylamide gel electrophoresis (SDS-PAGE) and transferred to polyvinylidene fluoride (PVDF) membranes (Millipore, Bedford, UK). The primary antibodies (1:1000) are shown in [Supporting Information Table S3](#). The membranes were applied with the corresponding HRP-conjugated secondary antibodies (Santa Cruz, Dallas, TX, USA) at 1:5000 dilutions for 1 h and then briefly incubated with ECL detection reagent (Amersham Biosciences, Castle Hill, Australia) to visualize the proteins before they were exposed on X-ray film.

2.10. Detection of hepatocyte growth factor (HGF) secretion

SKOV3 and SKOV3/T4 cell culture supernatants were collected after 72 h of incubation. HGF secretion levels from SKOV3 and

SKOV3/T4 cells in the suspension were detected with the Abcam Company HGF human enzyme-linked immunosorbent assay (ELISA) kit according to the operation requirements.

2.11. Cell viability assay

The anti-proliferative effects were measured by sulforhodamine B (SRB, Sigma–Aldrich) assay as described previously¹⁵. Cell proliferation rate was calculated according to Eq. (1):

$$\text{Cell proliferation rate (\%)} = \frac{A_{510} \text{ treated cells}}{A_{510} \text{ control cells}} \times 100 \quad (1)$$

2.12. Anti-tumor activity in vivo

The Animal Research Committee at Zhejiang University (Hangzhou, China) approved all animal studies, and animal care was provided in accordance with institutional guidelines. Six- to eight-week-old were utilized for the experiments (National Rodent Laboratory Animal Resource). Then, 1×10^6 SKOV3 and SKOV3/T4 cells were injected into the left and right armpits of the mice, respectively. When tumors reached a mean group size of approximately 100 mm^3 , the mice were randomly assigned to the following four groups: vehicle, adriamycin (1 mg/kg, i.p., qd; TargetMol, Boston, MA, USA), XL184 (20 mg/kg, i.g., qd; Selleck Chemicals, Huston, TX, USA) and XL184 (80 mg/kg, i.g., qd). During the experiment, body weight and tumor volume were regularly monitored. The inhibition ratio was calculated according to Eq. (2):

$$\text{Inhibitory ratio (\%)} = \left[\frac{\text{The average tumor weights of the model} - \text{the average tumor weights of treated groups}}{\text{The averagetumor weights of the model}} \right] \times 100 \quad (2)$$

2.13. Statistical analysis

All results were expressed as the mean \pm standard deviation (SD). For quantitative analysis, the experiments were repeated three times and the differences among means were significant determined by the Student's *t*-test or ANOVA test (* $P < 0.05$, ** $P < 0.01$, or *** $P < 0.001$).

3. Results

3.1. SKOV3/T4 subpopulation possessed enhanced migration activity

To enrich for cells with higher motility which mimic metastatic ovarian cancer cells, Transwell assays were repeated 4 times, and those cells that migrated into the lower chamber were collected and designated as the SKOV3/T4 subpopulation (Fig. 1A). Compared to the parental cells, the SKOV3/T4 subpopulation exhibited much a higher potential to migrate (Fig. 1B, C, and [Supporting Information Fig. S1A](#)). Since it is an important step for tumor metastasis to travel through blood vessels, we applied the chick embryo chorioallantoic membrane model to assess the motility of SKOV3/T4 cells. SKOV3/T4 cells migrated much more than parental SKOV3 cells (SKOV3/T0) cells (Fig. S1B and C). Interestingly, the SKOV3/T4 subpopulation displayed morphological changes from a cobblestone to a spindle-like morphology, which is a classical marker of EMT induction (Fig. S1D).

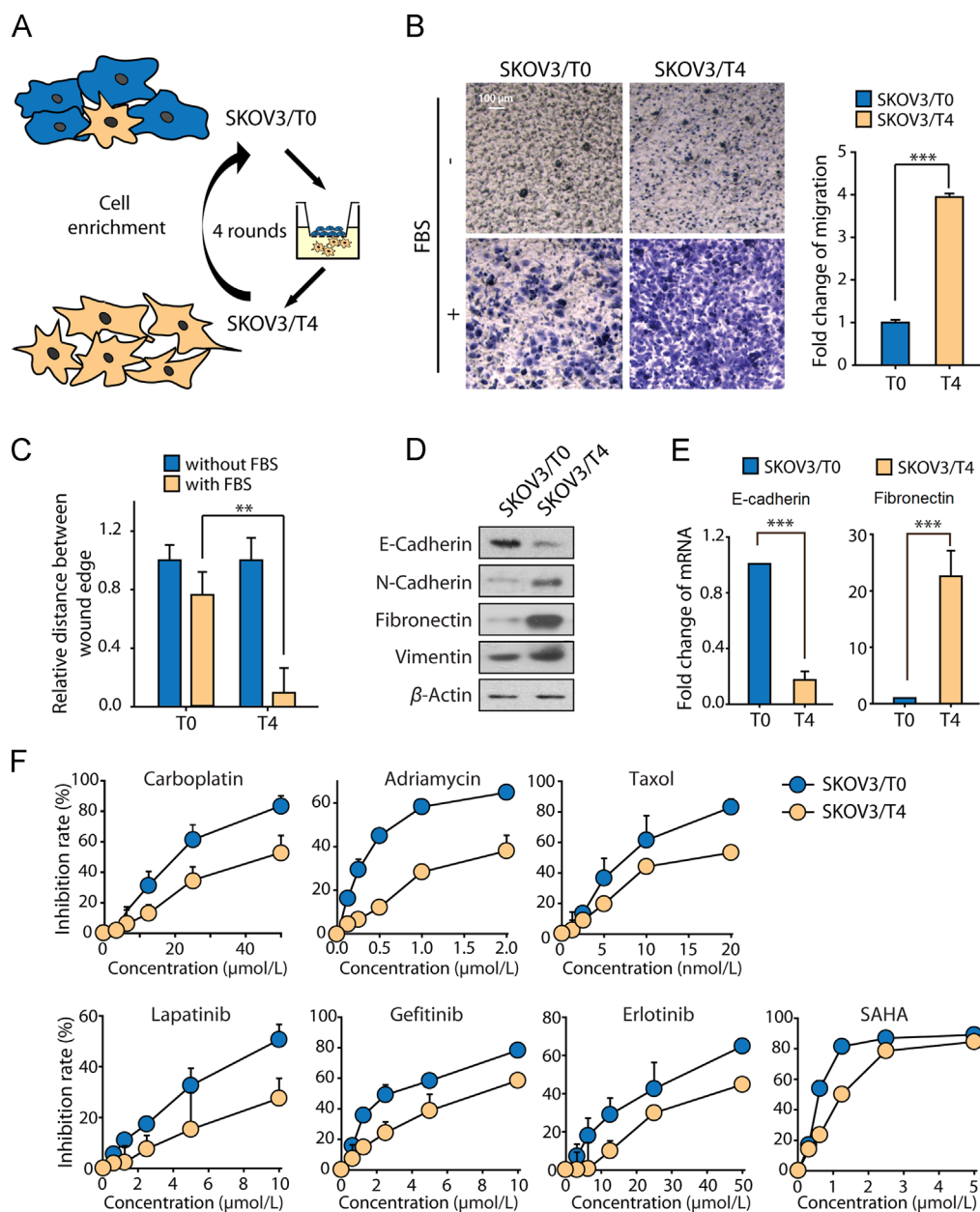


Figure 1 Enriched SKOV3/T4 subpopulation exhibited higher potency for migration and chemoresistance. (A) The SKOV3/T4 subline was established by reciprocal enrichment of SKOV3/T0 cells by collecting cells from the lower chamber of a transwell assay. SKOV3/T4 cells exhibited a significantly increased ability to migrate, as shown by (B) transwell assay and (C) wound-healing assay. The protein (D) and mRNA (E) levels of the epithelial marker E-cadherin was decreased while the mesenchymal markers were elevated in SKOV3/T4 cells. (F) The inhibition ratio of a variety of anti-cancer drugs on SKOV3/T0 and SKOV3/T4 cell lines. Statistical significance was determined by the Student's *t*-test (** $P < 0.01$ and *** $P < 0.001$).

Correspondingly, two TGF β factors, which are canonical upstream regulators of EMT, were predicted to be activated in SKOV3/T4 cells by microarray cluster analyses (Supporting Information Table S4). In this context, we aimed to evaluate the expression of markers in epithelial and mesenchymal phenotypes and found that E-cadherin protein expression was greatly decreased in SKOV3/T4 cells, while the levels of N-cadherin, fibronectin and vimentin were enhanced (Fig. 1D). Similar to the protein levels, mRNA levels of E-cadherin and fibronectin were downregulated and elevated (Fig. 1E), respectively. These findings collectively implicate that the enriched SKOV3/T4 subpopulation

from the parental SKOV3/T0 cells possess EMT properties and a high metastatic potential.

3.2. SKOV3/T4 subpopulation was resistant to chemotherapeutic agents

Mounting evidence has revealed the high correlation between metastasis and drug resistance¹⁶. The most important clinical evidence is that metastatic ovarian cancers almost lose the susceptibility to a large spectrum of anti-cancer drugs. Consequently, we determined the *in vitro* growth inhibitory effects of a

variety of anti-cancer drugs, including the three most commonly used chemotherapeutic agents for ovarian cancer patients (carboplatin, adriamycin and Taxol), as well as four targeted inhibitors (lapatinib, gefitinib, erlotinib and SAHA) against the SKOV3/T0 and SKOV3/T4 cell lines. As expected, the enriched SKOV3/T4 subpopulation with higher metastatic potential was resistant to the anti-cancer drugs as indicated by a decreased inhibition ratio and increased IC₅₀ values (Fig. 1F, Fig. S1E and F).

These data suggest that the metastatic SKOV3/T4 subpopulation is endowed with increasing resistance toward a panel of anti-cancer drugs including the most commonly used agents for ovarian cancer patients.

3.3. Slug overexpression decreased the susceptibility of SKOV3/T0 to anti-cancer drugs

The data suggested that the enriched metastatic SKOV3/T4 subpopulations were highly resistant to anti-cancer drugs. To explore the key factor(s) or mechanism(s) underlying the drug resistance, we monitored the mRNA profiles of parental, SKOV3/T2 (cells enriched twice from the lower chambers) and SKOV3/T4 cells. Because we were aiming to unravel the link between metastasis and drug resistance, the transcriptional factors involved in EMT were examined. Among these transcription factors, the mRNA levels of slug were elevated (Fig. 2A), which was verified by quantitative reverse transcription polymerase chain reaction (qRT-PCR, Fig. 2B). Our results also showed that slug protein levels were greatly increased in SKOV3/T4 cells, whereas other transcriptional factors, such as ZEB1, ZEB2 or snail, remained unchanged (Fig. 2C).

Exogenous introduction of slug caused morphological changes to the mesenchymal phenotype (Supporting Information Fig. 2A), occurrence of EMT (Fig. S2B) and enhanced motility (Fig. S2C) in SKOV3/T0 cells, which was in line with aforementioned data (Fig. 1B–E and Fig. S1A–D). Inversely, slug knockdown in SKOV3/T4 cells reversed the EMT process (Fig. S2D). To establish a link between slug and drug resistance in enriched metastatic SKOV3/T4 subpopulations, exogenous slug was introduced into parental SKOV3/T0 cells. We found that slug overexpression significantly increased the IC₅₀ values of carboplatin, adriamycin, Taxol, lapatinib, gefitinib and erlotinib (Fig. 2D), indicating that slug is fundamental for the decreased drug sensitivity in the SKOV3/T4 subpopulation.

Taken together, these data demonstrate that elevated slug transcription factor confers resistance to anti-cancer drugs in the SKOV3/T4 subpopulation.

3.4. c-Met activation in slug-positive cells played fundamental roles in the drug resistance

We have demonstrated the critical roles played by slug in drug resistance in the metastatic ovarian cancer subpopulation. This finding was consistent with several previous reports that slug conferred resistance to anti-cancer drugs^{12,14}; however, little is known about how to overcome this drug resistance mediated by slug. Thus, we prompted to investigate the signaling pathways activated by slug to explore effective interventions based on the molecular mechanisms by which slug-overexpressed tumors develop resistance to therapeutic agents.

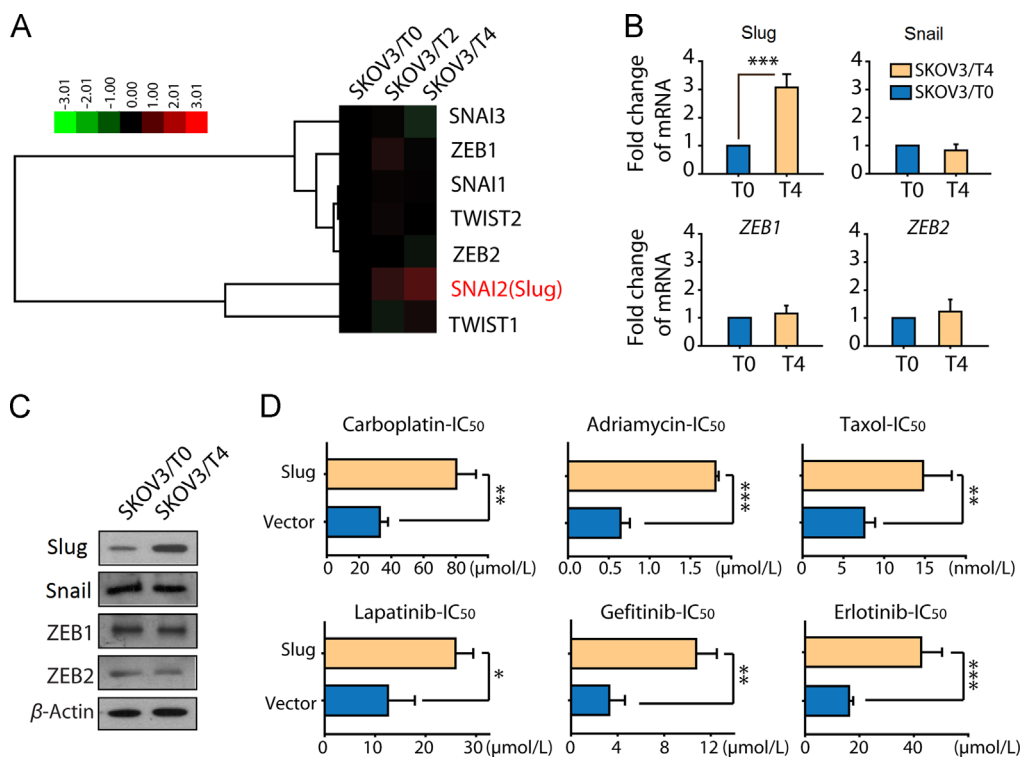


Figure 2 The higher expression of the transcription factor slug confers resistance to SKOV3/T4 cells. (A) mRNA array analysis revealed that the transcription factor slug was increased in SKOV3/T4 cells. (B) qRT-PCR analyses depicted the mRNA levels of the transcription factors slug, snail, ZEB1 and ZEB2. (C) The protein expression levels of EMT-related transcription factors in SKOV3/T0 parental and T4 sublines were determined. (D) Ectopic slug expression in SKOV3/T0 parental cells decreased the potency of anti-cancer agents. Statistical significance was determined by the Student's *t*-test (* $P < 0.05$, ** $P < 0.01$, and *** $P < 0.001$).

Recently, several lines of evidence implicate the aberrant activation of tyrosine kinase in the EMT transition process, which was accompanied by the upregulation of slug or its family members^{17–19}. In the attempt to determine which tyrosine kinase(s) would be activated in EMT-like SKOV3/T4 cells, we discovered the activation of c-Met, a trans-membrane receptor tyrosine kinase (RTK) (Fig. 3A). In contrast, the phosphorylation levels of other RTKs, including epidermal growth factor receptor (EGFR) and kinase insert domain receptor 2 (VEGFR2) in SKOV3/T4 cells, remained similar to that in SKOV3/T0 parental cells (Fig. 3B). The c-Met activation might be involved in slug-promoted migration and invasion, since XL-184, a small molecule kinase inhibitor against c-Met, could significantly hinder the motility of slug-overexpressing cells or SKOV3/T4 cells (Supporting Information Fig. S3A) while suppressing c-Met phosphorylation levels (Fig. S3B). The inhibitors against EGFR (gefitinib)^{20,21} and VEGFR (sunitinib)²² imposed no effects on the migration of SKOV3/T4 cells or SKOV3/T0 cells with ectopically transfected slug (Fig. S3C).

We next explored whether the activated c-Met in SKOV3/T4 cells was caused by slug overexpression. As shown in Fig. 3C, the phosphorylation of c-Met would be markedly impaired by slug knockdown; inversely, the ectopic expression of slug in SKOV3/T0 parental cells greatly activated c-Met phosphorylation. These findings established the causal link between slug overexpression and c-Met activation. We also studied whether c-Met activation could upregulate slug. Intriguingly, slug protein remained unchanged when treated with c-Met siRNA or XL184, suggesting that c-Met inhibition imposed minimal effect on slug levels (Fig. 3D). All these findings indicate that slug may be an upstream factor of the c-Met signalling pathway.

Based on the aforementioned evidence that slug-activated c-Met was critical for the increased motility of the SKOV3/T4 subpopulation, we speculated that activated c-Met due to slug may also contribute to drug resistance. To further test this possibility, we compared the cell viability of SKOV3/T0 and SKOV3/T4 in the presence of serial concentrations of XL184. Intriguingly, although SKOV3/T4 was endowed with resistance to most chemotherapy drugs (Fig. 1), these cells showed a much higher response to XL184 than SKOV3/T0 cells (Fig. 3E). Next, we introduced exogenous slug into SKOV3/T0 cells harboring lower expression levels of slug and p-Met and evaluated the drug efficiency in these cells. As expected, similar with the observations in SKOV3/T4 cells, both of the c-Met inhibitors we used, XL184 and PF-02341066, showed greatly enhanced cytotoxicity in slug-transfected SKOV3/T0 cells compared with the vector group (Fig. 3F). In order to further confirm the contribution of c-Met in the metastasis-associated drug resistance, c-Met siRNA was introduced. And we found that c-Met silence not only impaired the cell motility induced by slug overexpression, but also specifically increased the anti-cancer activities of adriamycin in resistant SKOV3/T4 cells, but not in parental SKOV3/T0 cells (Supporting Information Fig. S4). Altogether with the above-mentioned data (Fig. 2D) showing that the anti-cancer effects of carboplatin, adriamycin and other chemotherapeutic agents could be significantly attenuated by slug, these findings indicate that slug-mediated drug resistance could be overcome by c-Met inhibitors, thus demonstrating the functional importance of the c-Met pathway in slug-positive ovarian cancer cells.

To investigate the potential correlation of slug and p-Met in other cancer types, we further determined the cytotoxicity of XL184 as well as the slug protein levels in 9 different cancer cell

lines originating in the colon, lung, breast, liver, etc. Notably, as shown in Fig. 3G, the expression levels of slug were inversely correlated with the XL184 IC₅₀ values ($r = -0.66$), which was in line with our findings in ovarian cancer cells.

Collectively, these data suggest that c-Met is highly phosphorylated in SKOV3/T4 due to elevated slug levels in this metastatic subpopulation, making these slug-positive cells more susceptible to c-Met inhibitors.

3.5. Slug reinforced fibronectin-integrin αV (ITGA5) activity to induce c-Met phosphorylation and modulate the drug response

The aforementioned data revealed that slug overexpression resulted in the activation of c-Met through phosphorylation. It would be interesting to explore how slug, as a transcription factor, reinforces the phosphorylation of c-Met. Several lines of evidence have revealed that drug resistance can result from MET amplification or HGF-mediated Met activation^{23–26}. Thus, we first compared the mRNA levels of MET and HGF in the parental SKOV3/T0 cells and drug-resistant SKOV3/T4 subpopulation using qRT-PCR analysis and found that the mRNA levels of these two genes were similar in these two cell populations (Fig. 4A). Additionally, both cellular and secretory levels of HGF protein remained at similar levels in the SKOV3/T4 and SKOV3/T0 cells (Fig. 4B and C). These data ruled out the possibility that c-Met activation resulted from increased c-MET expression or ligand (HGF)-triggered signaling.

Consequently, we examined the mechanisms underlying HGF-independent activation of c-Met. Mitra et al.²⁷ reported that c-Met can also be activated in a ligand-independent manner through the activated ITGA5. Thus, we addressed whether the activated c-Met in SKOV3/T4 cells was induced by ITGA5. We interfered with ITGA5 expression in SKOV3/T4 cells using siRNA and found that ITGA5 depletion resulted in a dramatic decrease in c-Met phosphorylation in SKOV3/T4 cells (Fig. 4D). However, slug overexpression imposed few effects on ITGA5 expression (Supporting Information Fig. S5), implying that the function of ITGA5, rather than the protein level itself, contributed to c-Met activation.

Given that (1) ITGA5 function is regulated by the ligand fibronectin and (2) fibronectin is tightly modulated by slug through transcriptional activation, we speculated that c-Met phosphorylation in slug-positive cells might originate from slug-induced fibronectin and the subsequent fibronectin-ITGA5 interaction and activation. To confirm our hypothesis, we first examined the levels of fibronectin in slug-transfected SKOV3/T0 cells using an immunofluorescence assay. As shown in Fig. 4E, slug overexpression in SKOV3/T0 cells greatly upregulated fibronectin protein levels (Fig. 4E). This result was in line with our above-mentioned findings that the SKOV3/T4 subpopulation harbored much higher fibronectin protein and mRNA levels (Fig. 1D and E). We next raised a question whether the elevated fibronectin was critical for c-Met signaling by depleting fibronectin in SKOV3/T4 cells. Fig. 4F shows that c-Met phosphorylation was significantly ablated by fibronectin-targeting siRNAs, implicating the indispensable role of fibronectin in c-Met activation. Furthermore, we silenced ITGA5 in slug-transfected SKOV3/T0 cells, aiming to determine whether slug-fibronectin-elicited c-Met activation was mediated through ITGA5. As expected, slug overexpression greatly activated c-Met by phosphorylation, whereas ITGA5 interference completely abolished the p-Met levels induced by slug (Fig. 4G). Taken together, these results indicated that slug increased c-Met phosphorylation by activating fibronectin-ITGA5 in SKOV3/T4 cells.

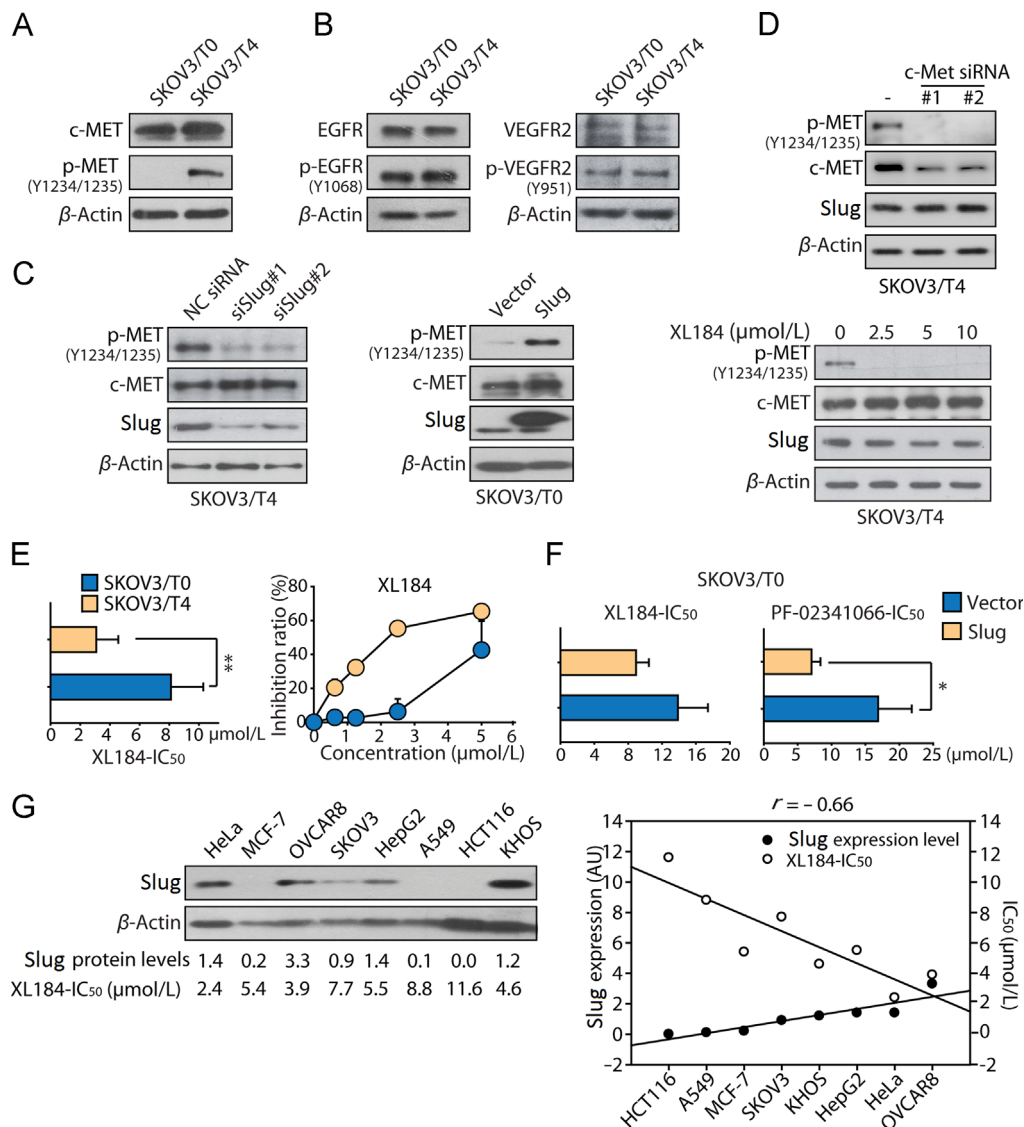


Figure 3 c-Met is highly phosphorylated in SKOV3/T4 cells and confers increased sensitivity to the Met inhibitor XL184. (A) The phosphorylation levels of c-Met were upregulated in the T4 subline. (B) The phosphorylation levels of EGFR and VEGFR2 in T4 cells were similar to that in SKOV3/T0 cells. (C) Depletion of slug in SKOV3/T4 cells attenuated the phosphorylation of c-Met, while ectopic slug expression in SKOV3/T0 cells enhanced p-Met levels. (D) The c-Met siRNA and the c-Met inhibitor XL184 could abrogate p-Met levels in SKOV3/T4 cells. (E) XL184 exhibited more potent anti-cancer activities on SKOV3/T4 cells. (F) Exogenous introduction of slug conferred parental SKOV3/T0 cells with a higher susceptibility to the c-Met inhibitors XL184 and PF-02341066. (G) Slug expression levels were inversely correlated with XL184 IC₅₀ values in a variety cancer cells. Statistical significance was determined by the Student's *t*-test (**P* < 0.05 and ***P* < 0.01).

To investigate whether the slug–ITGA5 axis participated in the drug resistance in slug-positive SKOV3/T4 cells promoted by elevated p-Met, we next evaluated the effects of depleting slug or ITGA5 on SKOV3/T4 cell drug sensitivity. As shown in Fig. 4H, slug silencing greatly enhanced the anti-proliferative effects of adriamycin and Taxol. This finding was in line with the aforementioned data that exogenous slug led to metastasis-associated drug resistance (Fig. 2D). In addition to slug knockdown, the deletion of ITGA5 also sensitized SKOV3/T4 cells to gefitinib and erlotinib (Fig. 4I).

Collectively, these data not only further confirm the link between slug, activated ITGA5 and phosphorylated c-Met, but also demonstrate the fundamental function of the slug–fibronectin–ITGA5–c-Met axis in modulating the drug response of SKOV3/T4 cells.

3.6. c-Met inhibition overcame adriamycin resistance and exerted potent *in vivo* anti-cancer activities in slug-positive SKOV3/T4 cells

To further investigate the differential *in vivo* activities of adriamycin (chemotherapeutic agent) and XL184 (c-Met inhibitor) in SKOV3/T0 and SKOV3/T4 cells, we employed subcutaneous xenografted tumor models (Fig. 5A) and implanted these two subpopulation into the left and right flanks, respectively. The mice bearing parental and metastatic SKOV3 cells were treated with vehicle, adriamycin (1 mg/kg) or XL184 (20/80 mg/kg) once a day for 15 days. Tumor volume (Fig. 5B) and body weight (Fig. 5C) were monitored every 2 days and p-MET as well as slug protein levels of these drug-treated SKOV3/T0 and SKOV3/T4 tumors were also evaluated (Fig. 5D). As shown in Fig. 5B and E, XL184 treatment exerted

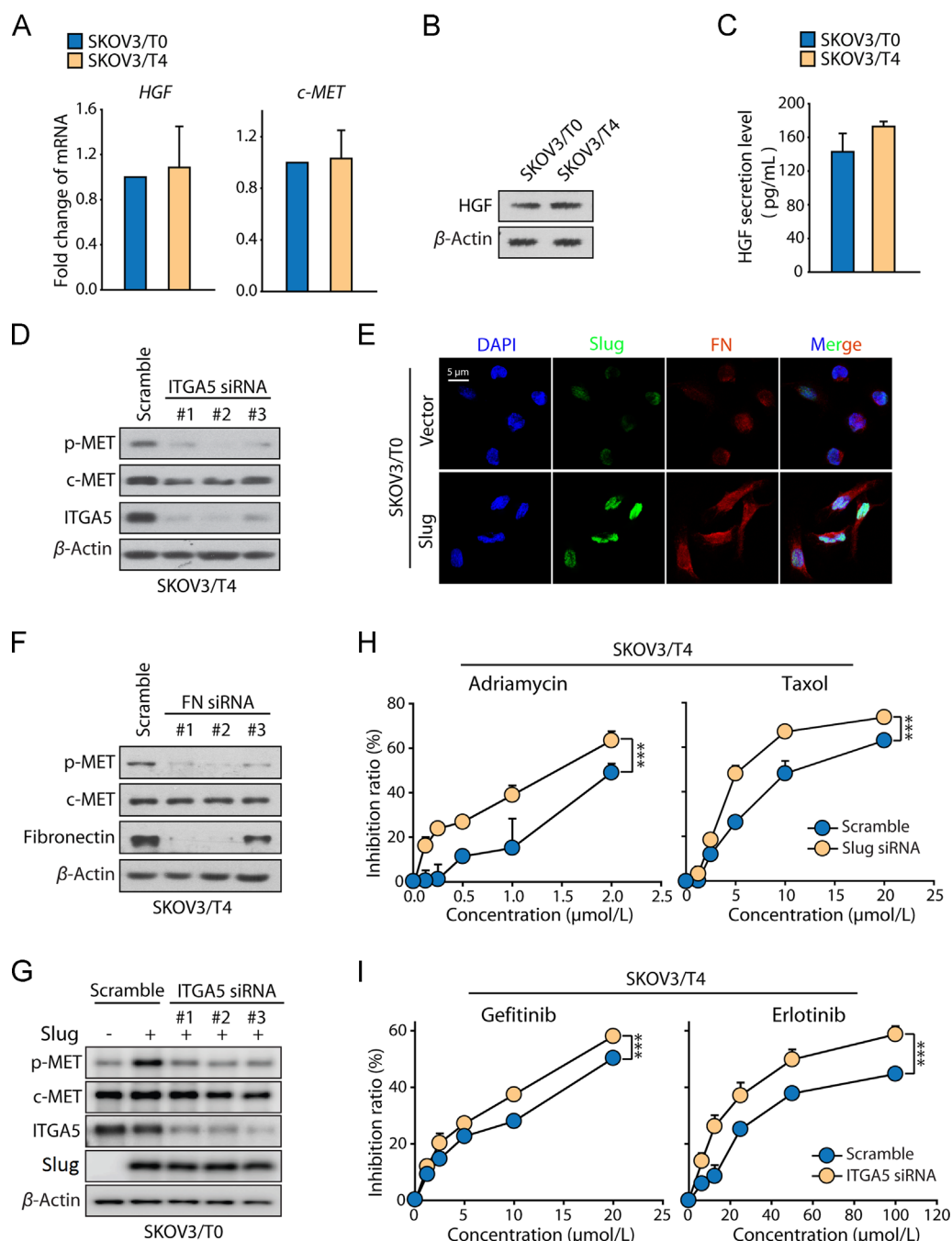


Figure 4 Slug induced the phosphorylation of c-Met by activating fibronectin–ITGA5. SKOV3/T4 cells harbored similar HGF mRNA (A) and protein (B) levels as the parental SKOV3/T0 cells. (C) SKOV3/T0 and SKOV3/T4 cells secreted comparable amounts of HGF in conditioned medium. (D) Silencing ITGA5 decreased c-Met phosphorylation in SKOV3/T4 cells. (E) Exogenous transfection of slug could greatly induce the cellular levels of fibronectin. (F) The depletion of fibronectin in SKOV3/T4 cells reduced c-Met phosphorylation. (G) ITGA5 knockdown abolished c-Met phosphorylation induced by exogenous transfection of slug in SKOV3/T0 cells. (H) Depletion of slug sensitized SKOV3/T4 cells to chemotherapeutic agents including adriamycin and Taxol. (I) ITGA5 silencing increased the anti-proliferative effects of gefitinib and erlotinib in SKOV3/T4 cells. Statistical significance was determined by ANOVA-test (***) $P < 0.001$.

significantly higher anti-cancer effects on SKOV3/T4 xenografted tumors than on SKOV3/T0 tumors. For example, at the 20 mg/kg dose, XL184 could exert strong suppressive effects on SKOV3/T4 tumors with minimal impact on animal body weight, as indicated by the inhibition rate of 64.3%. In contrast, in the same group of mice, XL184 failed to potently arrest the tumor growth of the parental SKOV3 tumors in the other flank side (inhibition rate of 37.5%). In

contrast, adriamycin treatment was much less effective on the SKOV3/T4-xenografted tumors than on the SKOV3/T0 tumors, and promoted evident body weight loss in mice. Fig. 5D further confirms the *in vivo* existence of the highly activated slug–c-Met axis on the SKOV3/T4 tumors.

Similar to the observations achieved with the cellular models, these findings implicate that due to the higher levels of the slug–c-Met axis,

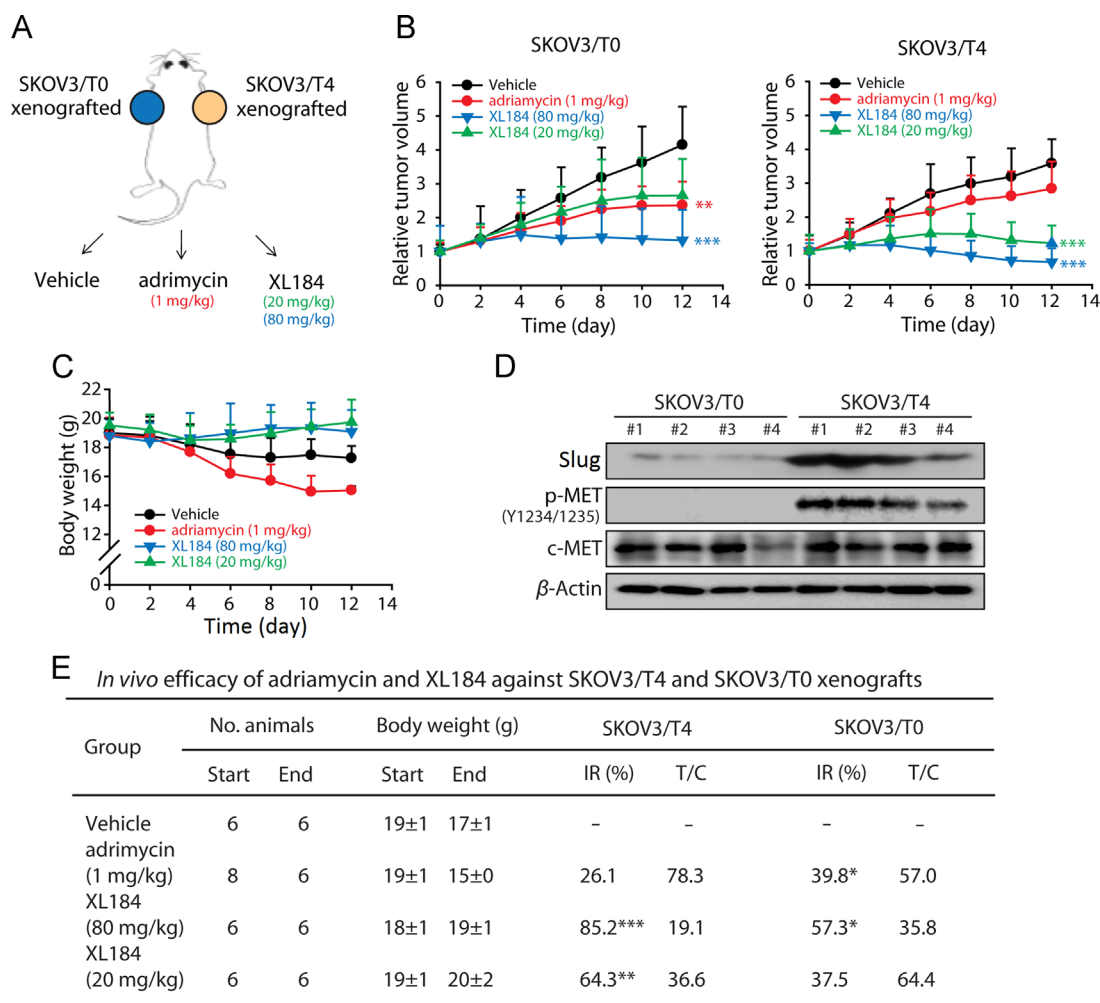


Figure 5 XL184 exerted superior anti-cancer activities in SKOV3/T4-xenografted tumors, which were highly resistant to adriamycin. (A) Equal amounts of SKOV3/T0 and SKOV3/T4 cells were injected subcutaneously into the left or right subaxillary of nude mice, respectively. The mice harboring both cell lines were administered adriamycin or XL184. (B) The relative tumor volumes of SKOV3/T0- and SKOV3/T4-xenografted tumors administered vehicle, adriamycin or XL184. (C) The body weights of the nude mice were significantly affected by adriamycin, but less affected by XL184. (D) WB analyses of xenografted tumors showed that SKOV3/T4 tumors harbored higher levels of slug and P-MET. (E) The inhibition ratio and T/C values of the adriamycin- and XL184-administered groups. Statistical significance was determined by the Student's *t*-test (* $P < 0.05$, ** $P < 0.01$ and *** $P < 0.001$).

XL184, a c-Met inhibitor, could exhibit more potent *in vivo* anti-cancer activities on the metastatic SKOV3/T4 subpopulation, which is highly resistant to chemotherapeutic agents used for ovarian cancer treatment.

3.7. Slug–c-Met axis associated with progression and poor prognosis of human ovarian cancer

To determine the clinical relevance of slug–c-Met hyperactivation in patients with ovarian cancer, we detected the expression levels of slug and phosphorylated c-MET by immunohistochemical analysis in tumor tissue samples collected from 121 ovarian cancer patients. As illustrated in Fig. 6A and B, the expression levels of slug were positively correlated with that of p-MET in these ovarian cancer samples ($R = 0.59$, $P < 0.01$), which supported the existence of the slug-induced activation of c-Met in ovarian cancer patient samples.

Furthermore, using Kaplan–Meier plotter analyses (<http://kmplot.com/analysis/>), we found that the slug mRNA levels in tumor tissues

were inversely correlated with progression-free survival (PFS), overall survival (OS) and postprogression survival (PPS) in ovarian cancer patients ($P = 0.0003$ for PFS, $P = 0.00017$ for OS, and $P = 0.00033$ for PPS) (Fig. 6C). In contrast, *HGF* mRNA levels were not correlated to the prognosis of these ovarian cancer patients ($P > 0.05$, Fig. 6D).

These data are in line with our aforementioned results, and collectively, these findings not only support the existence of slug-induced noncanonical activation of c-Met in ovarian cancer patients, but also highlight the functional importance of the slug–c-Met axis in modulating the drug response in those patients. We believe that targeting c-Met could be a promising therapeutic strategy for slug-positive ovarian patients who indeed suffer from poor prognosis.

4. Discussion

Drug resistance toward chemotherapeutic agents, including platinum, adriamycin, etc., accounts for the high mortality associated

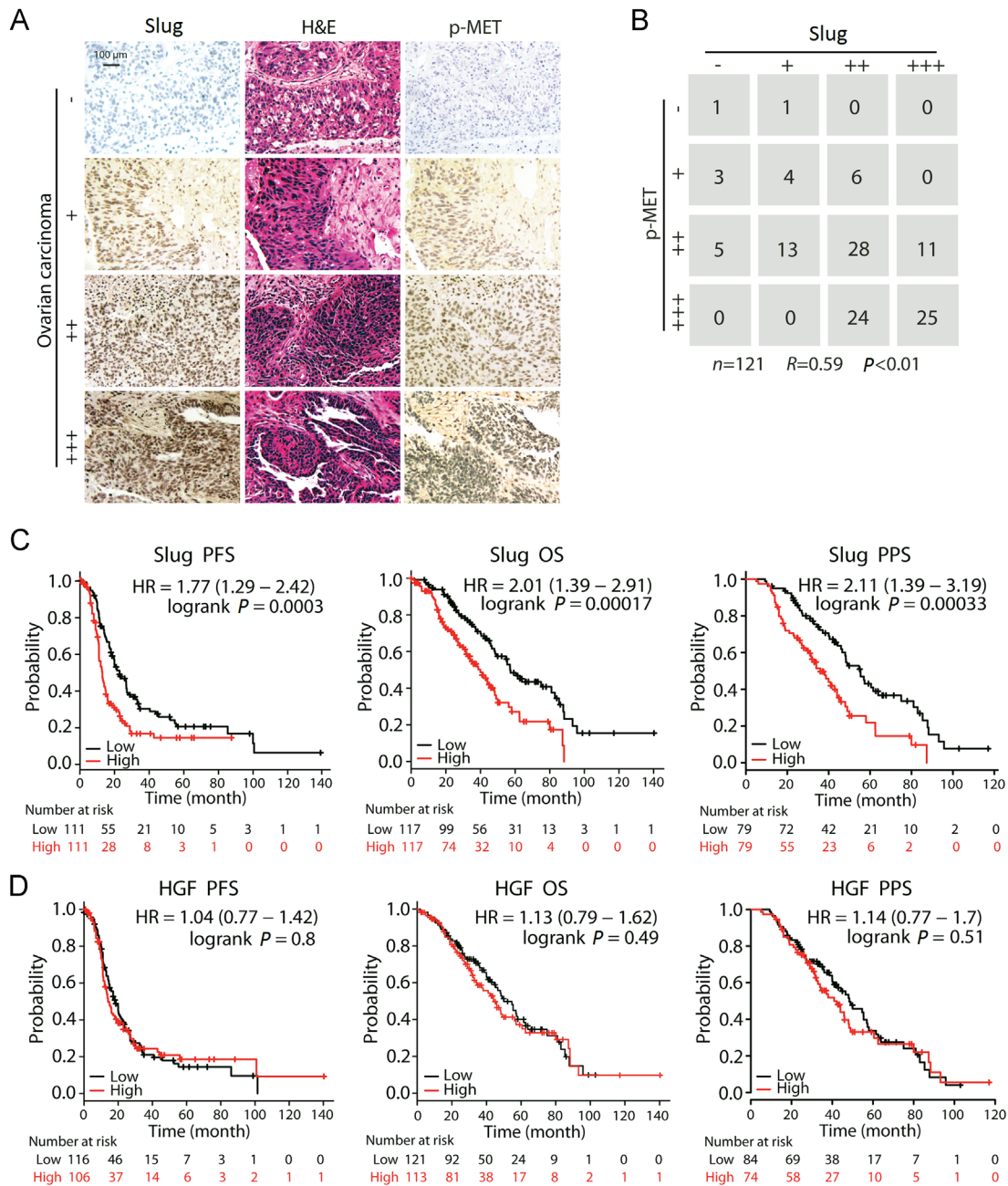


Figure 6 Slug protein expression was positively correlated with P-MET in tumor samples, predicting poor prognosis of ovarian cancer patients. (A) Tumor samples were obtained from 121 ovarian cancer patients and then subjected to in-parallel tissue staining for slug and P-MET. (B) Slug and P-MET expression levels were positively correlated in ovarian tumor samples. (C) Slug mRNA levels were correlated with PFS, OS and PPS in ovarian cancer patients (*P* < 0.001). (D) *HGF* mRNA levels were not associated with prognosis in ovarian cancer patients (*P* > 0.05).

with ovarian cancer, particularly metastatic ovarian cancer. Although there has been substantial progression in the development of targeting therapies, which have tremendously improved treatment outcomes for different cancer types, the survival rate of patients with ovarian cancer has changed little since platinum-based treatments were introduced more than 30 years ago¹. Mounting evidence shows that the major barrier for this treatment failure is the life-threatening drug resistance in ovarian cancer patients with metastasis. In this study, we found that the SKOV3/T4 subpopulation among SKOV3 ovarian cancer cells exhibited functional and phenotypic heterogeneity compared with the parental SKOV3 cells, including

significantly increased metastatic and resistant potential. This drug-resistant SKOV3/T4 subpopulation harbored higher expression levels of the transcription factor slug. Using gain- and loss-of-function approaches, we showed that elevated slug was required for SKOV3/T4 cell resistance to a panel of chemotherapeutic agents including platinum and adriamycin as well as EGFR inhibitors and HDAC inhibitors. Slug induced the fibronectin mRNA and protein levels, which bound to and activates IGTA5, leading to the subsequent noncanonical activation of the c-Met pathway in the SKOV3/T4 subpopulation. Our data showed that the hyperactivated slug-c-Met axis not only was fundamental for the

metastasis-associated drug resistance and poor prognosis associated with ovarian cancer but also opened an opportunity to kill these slug-positive resistant cells by interfering with c-Met function.

Slug is a member of the snail family. As an EMT-related gene, it potently promotes the induction of EMT through transcriptional reprogramming^{28–30}. Other EMT-related transcription factors including snail, twist, *ZEB-1*, etc. not only share the ability to induce EMT with slug but also possessed the function to modulate drug sensitivity in cancer cells. Several lines of evidence indicate that snail, twist, *ZEB-1* could promote drug resistance in different cancer models³¹. Nevertheless, in our current study, these EMT-related genes were not upregulated in the enriched EMT-like SKOV3/T4 cells, thus excluding their involvement in drug resistance in ovarian cancer cells.

Accumulating evidence has revealed that slug is correlated with the loss of anti-cancer activities by a variety of anti-cancer drugs in different cancer models. Chang et al.¹⁴ reported that slug could confer resistance to EGFR inhibitors in lung cancer by protecting cancer cells from apoptotic cell death. In colorectal cancer models, high slug expression could also modulate sensitivity to 5-fluorouracil by suppressing miR145³². Some reports suggested that slug could also function as a downstream factor of signaling cascades, demonstrating its involvement in FHIT-loss-mediated cisplatin resistance¹¹ or STAT3-mediated resistance to crizotinib³³. In accordance with these results, our findings show that slug is essential for drug resistance to different anti-cancer agents (Fig. 2D and H). Nevertheless, aside from using molecular manipulation on slug mRNA or protein expression, there are no clinically available therapeutic strategies against slug-mediated drug resistance.

In our current study, we identified the tyrosine kinase c-Met as the downstream effector that is activated by slug in ovarian cancer. Mechanistically, slug induced the mRNA expression of its target gene encoding fibronectin, which activates ITGA5, as fibronectin is a natural ligand for ITGA5. The interaction between fibronectin and ITGA5 could ultimately result in the activation of c-Met through phosphorylation in an HGF-independent manner (Fig. 4). This finding is in line with the previous report by Mitra et al.²⁷ that ITGA5 activated the c-Met pathway. Notably, this noncanonical c-Met activation offered a rational target for overcoming the slug-mediated drug resistance, as the present study provided *in vitro* and *in vivo* evidence that c-Met inhibitors exhibited superior anti-cancer activities in slug-positive ovarian cancer cells.

The c-Met signaling could be activated through canonical or noncanonical pathways. Canonical c-Met activation is induced by (1) the elevated c-Met or HGF expression levels^{24,25,34} or (2) increased HGF secretion^{35,36}. In the present study, although there was significant c-Met activation in SKOV3/T4 cells, neither elevated *c-MET* and *HGF* mRNA levels nor increased HGF secretion were observed, indicating the possibility that c-Met was activated in an HGF-independent manner in the drug-resistant SKOV3/T4 cells. This hypothesis was further supported by the Kaplan–Meier plotter analyses showing that *HGF* mRNA levels were not correlated with PFS, OS or PPS in ovarian cancer patients (Fig. 6D).

Several lines of evidence implicate that noncanonical c-Met activation is generally caused by the increased adhesion of cancer cells to the extracellular matrix, which involves the activation of ITGA5 or the other integrins. Subsequently, activated integrin could interact with c-Met, thus activating the latter to promote invasion and metastasis²⁷. However, to the best of our knowledge, the role of noncanonical c-Met signaling in modulating cellular sensitivity to anti-cancer drugs has not been explored. The present study showed

that slug activated c-Met in a noncanonical manner, and that slug mRNA levels were inversely correlated with survival time in ovarian cancer patients (Fig. 6C). Additionally, the slug–ITGA5–c-Met signaling cascade may play critical roles in metastasis-associated drug resistance to platinum or other chemotherapeutic agents in the SKOV3/T4 subpopulation or exogenous slug-transfected SKOV3/T0 cells. Conversely, c-Met-targeting by the small molecule inhibitor XL184 could inhibit the cell proliferation (*in vitro*) or tumor growth (*in vivo*) of the drug-resistant ovarian cancer cells more effectively (Figs. 3E–F and 5A–E). These findings underline the clinical and functional significance of noncanonical c-Met activation in ovarian cancer patients.

5. Conclusions

Using SKOV3/T4 cells, an enriched ovarian cancer subpopulation with high metastatic potential and remarkable drug resistance, we found an evident increase in slug expression. This elevated slug expression was essential for the EMT-like phenotype and migration ability, and also fundamental for the loss of drug sensitivity in ovarian cancer models to a variety of anti-cancer agents. Importantly, slug expression levels in tumor samples were highly correlated with poor prognosis in ovarian cancer patients, highlighting its clinical significance. We next established the causal link between slug overexpression and noncanonical c-Met activation, which endowed these slug-positive cells with enhanced susceptibility to c-Met-targeting agents. The superior anti-cancer activities of the c-Met inhibitor on SKOV3/T4 cells both *in vitro* and *in vivo* presents an opportunity to treat slug-positive-resistant ovarian cancer patients with c-Met-targeting strategies, which merit further clinical investigation in the future.

Acknowledgments

This work was supported by the National Natural Science Foundation for Distinguished Young Scholar of China (81625024 and 91529304, to Bo Yang), and National Natural Science Foundation of China (81673458, to Hong Zhu; 81503095, to Xiaoyang Dai), Zhejiang Provincial Natural Science Foundation (LY16H310004, to Xiaoyang Dai; China).

Appendix A. Supporting information

Supplementary data associated with this article can be found in the online version at <https://doi.org/10.1016/j.apsb.2019.03.001>.

References

- Vaughan S, Coward JI, Bast Jr RC, Berchuck A, Berek JS, Brenton JD, et al. Rethinking ovarian cancer: recommendations for improving outcomes. *Nat Rev Cancer* 2011;11:719–25.
- Holmes DA. Ovarian cancer: beyond resistance. *Nature* 2015;527:S217.
- Yap TA, Gerlinger M, Futreal PA, Pusztai L, Swanton C. Intratumor heterogeneity: seeing the wood for the trees. *Sci Transl Med* 2012;4:127ps110.
- Polyak K, Weinberg RA. Transitions between epithelial and mesenchymal states: acquisition of malignant and stem cell traits. *Nat Rev Cancer* 2009;9:265–73.

5. Ding Z, Wu CJ, Chu GC, Xiao Y, Ho D, Zhang J, et al. SMAD4-dependent barrier constrains prostate cancer growth and metastatic progression. *Nature* 2011;**470**:269–73.
6. Costa ET, Barnabe GF, Li M, Dias AA, Machado TR, Asprino PF, et al. Intratumoral heterogeneity of ADAM23 promotes tumor growth and metastasis through LGI4 and nitric oxide signals. *Oncogene* 2015;**34**:1270–9.
7. Tsai JH, Yang J. Epithelial-mesenchymal plasticity in carcinoma metastasis. *Genes Dev* 2013;**27**:2192–206.
8. Guan Xiangming. Cancer metastases: challenges and opportunities. *Acta Pharm Sin B* 2015;**5**:402–18.
9. Wang SP, Wang WL, Chang YL, Wu CT, Chao YC, Kao SH, et al. p53 controls cancer cell invasion by inducing the MDM2-mediated degradation of Slug. *Nat Cell Biol* 2009;**11**:694–704.
10. Kurrey NK, Amit K, Bapat SA. Snail and Slug are major determinants of ovarian cancer invasiveness at the transcription level. *Gynecol Oncol* 2005;**97**:155–65.
11. Wu DW, Lee MC, Hsu NY, Wu TC, Wang YC, Cheng YW, et al. FHT1 loss confers cisplatin resistance in lung cancer via the AKT/NF- κ B/Slug-mediated PUMA reduction. *Oncogene* 2017;**36**:5439.
12. Tsukasa K, Ding Q, Yoshimitsu M, Miyazaki Y, Matsubara S, Takao S. Slug contributes to gemcitabine resistance through epithelial-mesenchymal transition in CD133⁺ pancreatic cancer cells. *Hum Cell* 2015;**28**:167–74.
13. Jiang Y, Zhao X, Xiao Q, Liu Q, Ding K, Yu F, et al. Snail and Slug mediate tamoxifen resistance in breast cancer cells through activation of EGFR-ERK independent of epithelial-mesenchymal transition. *J Mol Cell Biol* 2014;**6**:352–4.
14. Chang TH, Tsai MF, Su KY, Wu SG, Huang CP, Yu SL, et al. Slug confers resistance to the epidermal growth factor receptor tyrosine kinase inhibitor. *Am J Respir Crit Care Med* 2011;**183**:1071–9.
15. Wang DD, Chen Y, Chen ZB, Yan FJ, Dai XY, Ying MD, et al. CT-707, a novel FAK inhibitor, synergizes with cabozantinib to suppress hepatocellular carcinoma by blocking cabozantinib-induced FAK activation. *Mol Cancer Ther* 2016;**15**:2916–25.
16. Bozic I, Nowak MA. Timing and heterogeneity of mutations associated with drug resistance in metastatic cancers. *Proc Natl Acad Sci U S A* 2014;**111**:15964–8.
17. Zhang K, Corsa CA, Ponik SM, Prior JL, Pivnicka-Worms D, Eliceiri KW, et al. The collagen receptor discoidin domain receptor 2 stabilizes SNAIL1 to facilitate breast cancer metastasis. *Nat Cell Biol* 2013;**15**:677–87.
18. Claperon A, Mergey M, Nguyen Ho-Bouidoires TH, Vignjevic D, Wendum D, Chretien Y, et al. EGF/EGFR axis contributes to the progression of cholangiocarcinoma through the induction of an epithelial-mesenchymal transition. *J Hepatol* 2014;**61**:325–32.
19. Reichl P, Dengler M, van Zijl F, Huber H, Fuhrlinger G, Reichel C, et al. Axl activates autocrine transforming growth factor- β signaling in hepatocellular carcinoma. *Hepatology* 2015;**61**:930–41.
20. Wen W, Wu J, Liu L, Tian Y, Buettner R, Hsieh MY, et al. Synergistic anti-tumor effect of combined inhibition of EGFR and JAK/STAT3 pathways in human ovarian cancer. *Mol Cancer* 2015;**14**:100.
21. Ciardiello F, Tortora G. EGFR antagonists in cancer treatment. *N Engl J Med* 2008;**358**:1160–74.
22. Jain RK. Antiangiogenesis strategies revisited: from starving tumors to alleviating hypoxia. *Cancer Cell* 2014;**26**:605–22.
23. Peters S, Adjei AA. MET: a promising anticancer therapeutic target. *Nat Rev Clin Oncol* 2012;**9**:314–26.
24. Turke AB, Zejnullahu K, Wu YL, Song Y, Dias-santagata D, Lifshits E, et al. Preexistence and clonal selection of MET amplification in EGFR mutant NSCLC. *Cancer Cell* 2010;**17**:77–88.
25. Engelman JA, Zejnullahu K, Mitsudomi T, Song Y, Hyland C, Park JO, et al. MET amplification leads to gefitinib resistance in lung cancer by activating ERBB3 signaling. *Science* 2007;**316**:1039–43.
26. Straussman R, Morikawa T, Shee K, Barzily-Rokni M, Qian ZR, Du J, et al. Tumour micro-environment elicits innate resistance to RAF inhibitors through HGF secretion. *Nature* 2012;**487**:500–4.
27. Mitra AK, Sawada K, Tiwari P, Mui K, Gwin K, Lengyel E. Ligand-independent activation of c-Met by fibronectin and $\alpha_5\beta_1$ -integrin regulates ovarian cancer invasion and metastasis. *Oncogene* 2011;**30**:1566–76.
28. Ye X, Tam WL, Shibue T, Kaygusuz Y, Reinhardt F, Ng Eaton E, et al. Distinct EMT programs control normal mammary stem cells and tumour-initiating cells. *Nature* 2015;**525**:256–60.
29. Fang JH, Zhou HC, Zhang C, Shang LR, Zhang L, Xu J, et al. A novel vascular pattern promotes metastasis of hepatocellular carcinoma in an epithelial-mesenchymal transition-independent manner. *Hepatology* 2015;**62**:452–65.
30. Liu X, Sun H, Qi J, Wang L, He S, Liu J, et al. Sequential introduction of reprogramming factors reveals a time-sensitive requirement for individual factors and a sequential EMT-MET mechanism for optimal reprogramming. *Nat Cell Biol* 2013;**15**:829–38.
31. Kaufhold S, Bonavida B. Central role of Snail1 in the regulation of EMT and resistance in cancer: a target for therapeutic intervention. *J Exp Clin Cancer Res* 2014;**33**:62.
32. Findlay VJ, Wang C, Nogueira LM, Hurst K, Quirk D, Ethier SP, et al. SNAI2 modulates colorectal cancer 5-fluorouracil sensitivity through miR145 repression. *Mol Cancer Ther* 2014;**13**:2713–26.
33. Cuyas E, Perez-Sanchez A, Micol V, Menendez JA, Bosch-Barrera J. STAT3-targeted treatment with silibinin overcomes the acquired resistance to crizotinib in ALK-rearranged lung cancer. *Cell Cycle* 2016;**15**:3413–8.
34. Coughnour A, Dalmasso G, Martinez R, Buc E, Delmas J, Gibold L, et al. Bacterial genotoxin colibactin promotes colon tumour growth by inducing a senescence-associated secretory phenotype. *Gut* 2014;**63**:1932–42.
35. Kang JY, Dolled-Filhart M, Ocal IT, Singh B, Lin CY, Dickson RB, et al. Tissue microarray analysis of hepatocyte growth factor/Met pathway components reveals a role for Met, matrilysin, and hepatocyte growth factor activator inhibitor 1 in the progression of node-negative breast cancer. *Cancer Res* 2003;**63**:1101–5.
36. Huang FI, Chen YL, Chang CN, Yuan RH, Jeng YM. Hepatocyte growth factor activates Wnt pathway by transcriptional activation of LEF1 to facilitate tumor invasion. *Carcinogenesis* 2012;**33**:1142–8.